

## A Self-Organizing Memory Neural Network for Aerosol Concentration Prediction

Qiang Liu<sup>1,\*</sup>, Yanyun Zou<sup>2,3</sup> and Xiaodong Liu<sup>4</sup>

**Abstract:** Haze-fog, which is an atmospheric aerosol caused by natural or man-made factors, seriously affects the physical and mental health of human beings. PM<sub>2.5</sub> (a particulate matter whose diameter is smaller than or equal to 2.5 microns) is the chief culprit causing aerosol. To forecast the condition of PM<sub>2.5</sub>, this paper adopts the related meteorological data and air pollutes data to predict the concentration of PM<sub>2.5</sub>. Since the meteorological data and air pollutes data are typical time series data, it is reasonable to adopt a machine learning method called Single Hidden-Layer Long Short-Term Memory Neural Network (SSHL-LSTMNN) containing memory capability to implement the prediction. However, the number of neurons in the hidden layer is difficult to decide unless manual testing is operated. In order to decide the best structure of the neural network and improve the accuracy of prediction, this paper employs a self-organizing algorithm, which uses Information Processing Capability (IPC) to adjust the number of the hidden neurons automatically during a learning phase. In a word, to predict PM<sub>2.5</sub> concentration accurately, this paper proposes the SSHL-LSTMNN to predict PM<sub>2.5</sub> concentration. In the experiment, not only the hourly precise prediction but also the daily longer-term prediction is taken into account. At last, the experimental results reflect that SSHL-LSTMNN performs the best.

**Keywords:** Haze-fog, PM<sub>2.5</sub> forecasting, time series data, machine learning, long short-term memory neural network, self-organizing algorithm, information processing capability.

### 1 Introduction

PM<sub>2.5</sub> (a particulate matter whose diameter is smaller than or equal to 2.5 microns) is one of the most critical factors for haze-fog formation. PM<sub>2.5</sub> emissions can be divided into primary pollution sources and secondary pollution sources. The primary pollution sources are mainly PM<sub>2.5</sub> particles produced directly by the combustion of fossil fuels (petroleum, coal, etc.), biomass fuels (straw, wood), dust and so on. Secondary pollution sources are

---

<sup>1</sup> School of Computer, Hunan University of Technology, Zhuzhou, China.

<sup>2</sup> Jiangsu Collaborative Innovation Center of Atmospheric Environment and Equipment Technology (CICAET), Nanjing University of Information Science & Technology, Nanjing, China.

<sup>3</sup> School of Computer & Software, Nanjing University of Information Science & Technology, Nanjing, China.

<sup>4</sup> School of Computing, Edinburgh Napier University, UK.

\* Corresponding Author: Qiang Liu. Email: liuqiang@hut.edu.cn.

mainly PM<sub>2.5</sub> particles produced by the combination of volatile organic compounds (VOCs), nitrogen oxides, sulfur dioxide, hydrocarbon organic compounds, nitrates and other particles in the atmosphere through chemical reactions. In the case of relatively stable pollution sources, meteorological conditions play a role in promoting the formation of haze. For example, Inverse temperature has a great influence on the formation of haze. Once the inversion stratification is formed, the air cannot convection up and down, so the pollutants are difficult to diffuse and accumulate continuously, which leads to the accumulation of PM<sub>2.5</sub>. In addition, the dilution of pollutants depends on the wind speed. If the wind speed is small, the pollutants are not easy to diffuse; but if the wind speed is too large, the dust on the ground will make the pollution more serious. Therefore, not only pollutants but also meteorological conditions have great influence on the formation of PM<sub>2.5</sub>.

Statistical methods played important roles in early PM<sub>2.5</sub> prediction field. Fuller et al. [Fuller, Carslaw and Lodge (2002)] explored the linear correlation factors with PM<sub>2.5</sub> through linear regression method, and then used these factors to predict PM<sub>2.5</sub>. Jian et al. [Jian, Zhao, Zhu et al. (2012)] found some related meteorological factors, such as humidity and wind speed by Auto-Regressive Integrated Moving Average (ARIMA) model. Dong et al. [Dong, Yang and Kuang (2009)] predicted PM<sub>2.5</sub> concentration using the hidden Markov function. The prediction results showed that the fitting effect between the predicted value and the real value are good.

To improve the accuracy of prediction, machine learning methods have been widely used in this field. Mishra et al. [Mishra, Goyal and Upadhyay (2015)] used multilayer perceptron model to predict haze-fog with pollution parameters (CO, O<sub>3</sub>, NO<sub>2</sub>, SO<sub>2</sub>, PM<sub>2.5</sub>) and meteorological parameters. Zheng et al. [Zheng and Shang (2013)] used the Radial Basis Function (RBF) neural network to predict the concentration of PM<sub>2.5</sub>. The results proved that compared with Back Propagation (BP), the prediction performance was better. In addition, some researchers adopt some optimization methods into machine learning methods. Liu et al. [Liu and Li (2015)] used the comprehensive prediction model to forecast the PM<sub>2.5</sub> concentration using the Auto-Regressive Moving Average (ARMA), Artificial Neural Networks (ANNs) model and Exponential Smoothing Method (ESM). Wang et al. [Wang, Liu, Chao et al. (2018)] introduced ARIMA and Support Vector Machine (SVM) to predict nonlinear time series data. Zhu et al. [Zhu and Lu (2016)] put forward an improved BP neural network algorithm, combining the ARMA model with BP neural network to predict PM<sub>2.5</sub> concentration. Venkadesha et al. [Venkadesh, Hoogenboom and Potter (2013)] combined genetic algorithm and BP neural network to improve the accuracy of prediction.

However, all of the above researches used feed-forward neural network without circulating loops for prediction. This kind of neural network is not able to memory history data to predict future data because of the one-direction architecture. Meteorological data and pollution data are typical time series data, the data of future moments are strongly correlated with those of historical moments. On the basis of feedforward neural network, another machine learning model called Reucurrent Neural Network (RNN) adds a self-feedback loop, which can effectively remember the historical time data. So many researchers adopted RNN to predict time series data. Zhou et al. [Zhou, Li and Qiao (2017)] used RNN to predict PM<sub>2.5</sub> concentration. Compared with Fuzzy Neural Network (FNN)

and RBF feedforward neural network, the experimental results show that RNN is outstanding. Bun et al. [Bun, Komei, Koji et al. (2016)] put forward a new training method for automatic encoder, which is designed for time series prediction, to enhance the RNN. The experiment shows that RNN is better than the typical and most advanced automatic coder training method used in the time series prediction.

From the above literatures, RNN (recurrent neural network) shows an excellent performance on predicting time series data due to its memory capability of historical information. However, when the value of connection weights is less than 1, the gradient may disappear. At this time, no matter what numerical operation is performed on the gradient, the parameters cannot be updated by gradient. At this time, Long Short-Term Memory (LSTM) neural network is proposed to change the network structure of RNN to overcome this defect. Tsai et al. [Tsai, Zeng and Chang (2018)] adopted LSTM neural network to forecast PM<sub>2.5</sub> concentration for next four hours in Taiwan. It was proved that used the LSTM neural network than the ANNs could had a better accuracy. Verma et al. [Verma, Ahuja, Meisheri et al. (2018)] used Bidirectional Long Short-Term memory (BiLSTM) to predict PM<sub>2.5</sub> concentration. Through comparison experiment, BiLSTM model shows superiority over Multi-Layer Perceptron (MLP).

However, how to decide the structure of the neural network, especially the number of hidden nodes, is still a problem worth discussing. Many researchers have done a lot of work to solve this problem using self-organizing algorithm. Subrahmanya et al. [Subrahmanya and Shin (2010)] adopted a growing method combined particle swarm optimization (PSO) algorithm to adjust the number of hidden nodes during the learning phase. Park [Park (2013)] used a pruning method which applied genetic algorithm (GA) to achieve the best structure of the neural network. However, in order to explore optimal ways to adjust the structure of the neural network, many researchers came up with hybrid methods which combined growing and pruning algorithms. Vukovica et al. [Vukovic and Miljkovic (2013)] employed the concept of neuron's significance to add or remove the neurons during the learning phase. Wang et al. [Wang, Ma, Wang et al. (2013)] used another concept, fitness function, to increase or decrease the number of neurons. Many researchers have put forward other growing and pruning methods and have been making progress in this field [El-Sousy (2014); Hsu (2014); El-Sousy and Khaled (2016); El-Sousy and Khaled (2018); Han, Zhang, Hou et al. (2016)].

According to the above literatures, owing to the typical time series character of air pollutants and meteorological data, this paper uses a machine learning method, which is an improved recurrent neural network called a Self-organizing Single Hidden-Layer Long Short-Term Memory Neural Network (SSHL-LSTMNN) to predict PM<sub>2.5</sub> concentration.

## **2 Methodology**

### ***2.1 Long short-term memory (LSTM) neural network***

Bengio et al. [Bengio, Simard and Frasconi (1994)] reported that RNNs are severely affected by gradient vanishing and gradient explosion problem. Thus, Hochreiter and Schmidhuber [Hochreiter and Schmidhuber (1997)] proposed a special RNN, called LSTM neural network, to overcome this problem.

For RNN, a layer of sigmoid passes through the hidden state of the front and back steps, so the gradient multiplies the derivative of a sigmoid when propagating backward; for LSTM, the hidden cell of the front and back steps does not pass through a sigmoid layer, but multiplies the function value of a sigmoid (that is, the forget gate of LSTM), so the gradient multiplies the function value of the last sigmoid instead of its derivative when propagating backward. So, RNN's gradient is the derivative multiplied by sigmoid in backward direction, LSTM's gradient is the function value multiplied by sigmoid in backward direction, and there is a significant difference between the numerical distribution of RNN's gradient and that of LSTM's gradient.

Therefore, in RNN, every time the derivative of sigmoid is multiplied, the gradient of backward propagation will be attenuated once, which needs to be pulled back by the matrix of the full connection layer, but if it is pulled too far, it will cause the gradient explosion, and if the variance in front of sigmoid is large, the gradient will disappear directly, and the whole connection layer will not be rescued; in LSTM, every time the function value of sigmoid is multiplied. The gradient of backward propagation can be retained or attenuated, which is very flexible. Moreover, the front and back hidden cells can take the "forget gate" shortcut directly without passing through the full connection layer, which is the root of gradient explosion, so LSTM does not need to worry about gradient explosion on this path. Fig. 1 displays the structure of LSTM block.

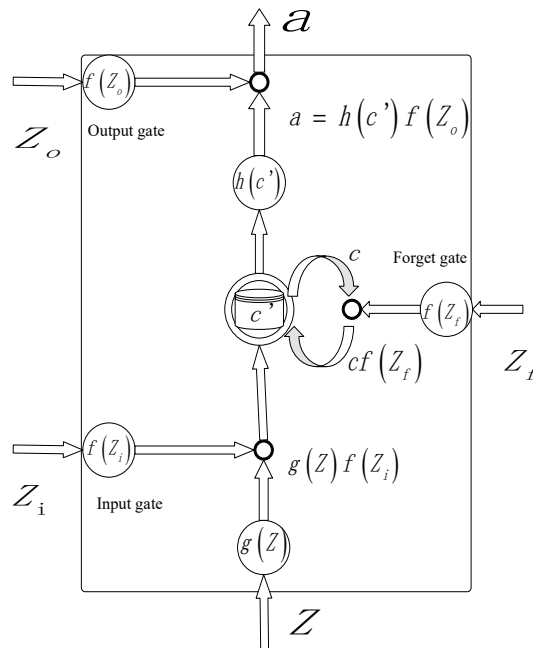


**Figure 1:** Structure of LSTM block

There are input gate, forget gate and output gate in the block.  $Z$  is the input data,  $Z_i$ ,  $Z_f$ ,  $Z_o$  are control signals. When  $f(Z_i) = 1$ ,  $g(Z)$  can be input. Instead, when  $f(Z_i) = 0$ ,

$g(Z)$  is not able to be input. Similarly,  $f(Z_o)$  controls the output of value.  $f(Z_f) = 1$  means the previous value  $C$  can be stored in memory cell. Then, when  $f(Z_f) = 0$ , it is equivalent to forget value  $C$ . Value  $C$  is updated as:

$$c' = g(Z) f(Z_i) + cf(Z_f) \tag{1}$$

In fact, LSTM neural network is to replace the hidden layer neurons of RNN with LSTM block. Fig. 2 shows the structure of single hidden-layer LSTM neural network.

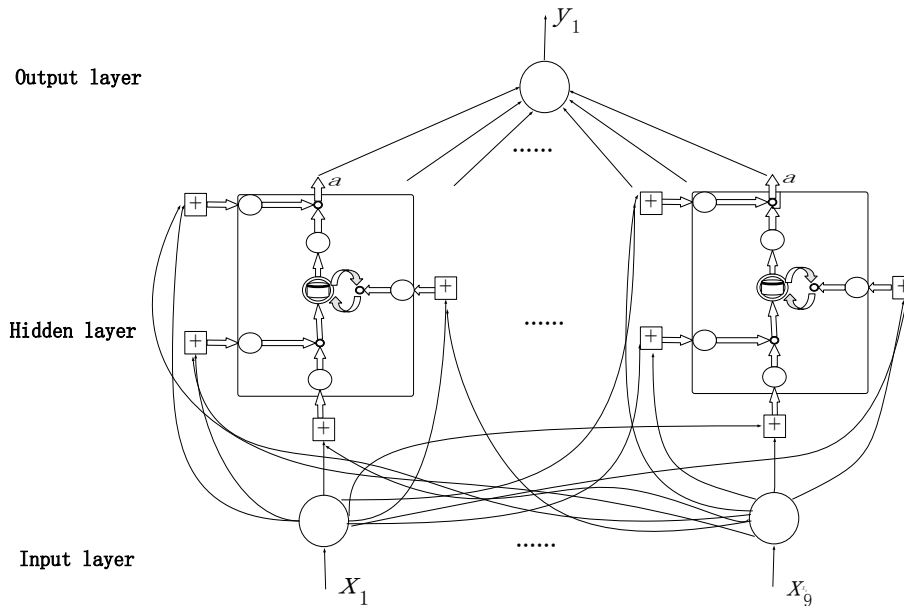


**Figure 2:** Structure of single hidden-layer LSTM neural network

There are input layer, hidden layer and output layer, and the number of input parameters is four times that of simple RNN. Though the structure becomes more complicated, the memory capability becomes more powerful.

Because the gradient vanishing and gradient explosion problems are usually occurred in deep neural network, so the simple neural network generally does not have such problems. In this paper, a single hidden layer LSTM neural network is adopted to predict concentration of PM<sub>2.5</sub>, which is a simple network structure. The self-organizing algorithm is only to adjust the number of hidden nodes instead of changing the method of weight optimization. Based on the above analysis, LSTM neural network can effectively avoid the gradient vanishing and gradient explosion problems. In a word, there are no gradient vanishing and gradient explosion problems in the single hidden layer LSTM neural network this paper used.

## 2.2 Information processing capability evaluation

In this paper, the number of hidden nodes in the SSHL-LSTMNN is adjusted by a self-organizing algorithm during training phase. In this algorithm, a crucial concept, Information Processing Capability (IPC), is adopted to add or delete the nodes of the hidden layer [Han, Guo and Qiao (2017)].

According to general properties of the neural network, the output of the hidden layer, as well as the output of the output layer can be presented as

$$\phi(t) = [\theta(t - K + 1), \dots, \theta(t - 1), \theta(t)]^T \quad (2)$$

The connection weights between the hidden layer and the output layer can be presented as

$$\delta(t) = [\omega(t - K + 1), \dots, \omega(t - 1), \omega(t)] \quad (3)$$

The output of the output layer can be presented as

$$y(t) = \phi(t) \delta(t) \quad (4)$$

IPC is able to express the independent component contribution between hidden nodes, as well as the contribution from the hidden nodes to output nodes. The expression of IPC is as follows:

$$\mathbf{Q}(t) = \Phi(t) \mathbf{W}(t) \quad (5)$$

$$\mathbf{Q}(t) = \begin{bmatrix} q_1(t - K + 1) & q_1(t - K + 2) & \cdots & q_1(t) \\ q_2(t - K + 1) & q_2(t - K + 2) & \cdots & q_2(t) \\ \vdots & \vdots & \vdots & \vdots \\ q_m(t - K + 1) & q_m(t - K + 2) & \cdots & q_m(t) \end{bmatrix} \quad (6)$$

$\mathbf{Q}(t) = [q_1(t), \dots, q_{j-1}(t), q_m(t)]^T$  is the independent contribution matrix,  $q_j(t) = [q_j(t - K + 1), \dots, q_j(t - 1), q_j(t)]$  is the independent contribution of the  $j_{th}$  hidden neuron,  $j = 1, \dots, m$ ,  $\mathbf{W}(t)$  is a coefficient matrix.

According to the above analysis, independent component contribution from hidden nodes to output nodes can be defined as

$$I_j(t) = \frac{\sum_{k=1}^K q_j(t - k + 1)}{\sum_{k=1}^K \sum_{j=1}^m q_j(t - k + 1)}, k = 1, \dots, K; j = 1, \dots, m, \quad (7)$$

## 2.3 Self-organizing algorithm

The growing and pruning algorithm is to add or delete hidden layer nodes by using IPC to

achieve self-organizing ability of the single hidden-layer LSTM network during learning phase. So the structure of the network is able to satisfy the high precision prediction condition. Fig. 3 displays the logical scheme of the growing and pruning algorithm.

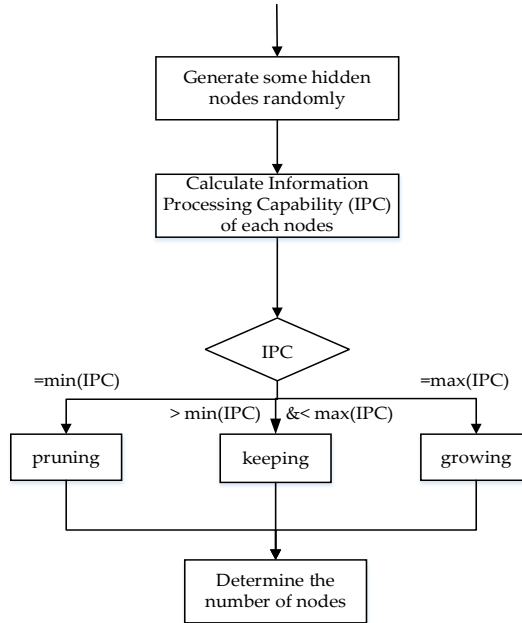


**Figure 3:** Logical scheme of the growing and pruning algorithm

The calculation of IPC is divided into two parts: the input IPC and output IPC, which are defined as:

$$\begin{cases} S_j^1(t) = \frac{1}{K} \sum_{k=1}^K e^{-\mathbf{x}(t-k+1)} \\ S_j^2(t) = I_j(t) \end{cases} \quad (8)$$

$\mathbf{x}(t - K + 1)$  is the input vector at time  $(t - K + 1)$ . The self-organizing algorithm contains three steps: growing step, pruning step and keeping step. The detailed process of each step is described below.

**Growing Step.** The larger  $S_j^1(t)$  and  $S_j^2(t)$  are, the information processing ability of the node is more powerful. In this case, if the IPC satisfies the following conditions:

$$\begin{cases} S_j^1(t) = \max S^1(t) \\ S_j^2(t) = \max S^2(t) \end{cases} \quad (9)$$

$S^1(t) = (S_1^1(t), \dots, S_{m-1}^1(t), S_m^1(t))$  and  $S^2(t) = (S_1^2(t), \dots, S_{m-1}^2(t), S_m^2(t))$  are input IPC vector and output IPC vector of hidden nodes respectively. If the input IPC

vector of a node is the maximum value among all input IPC vectors, and the output IPC vector is the maximum value among all output IPC vectors, a new hidden node will be inserted into the hidden layer. The connection weights of this node will be initialized.

**Pruning Step.** Like the above step, if the IPC of a node satisfies the following conditions:

$$\begin{cases} S_i^1(t) = \min S^1(t) \\ S_i^2(t) = \min S^2(t) \end{cases} \quad (10)$$

If the input IPC vector of a node is the minimum value among all input IPC vectors, and the output IPC vector is the minimum value among all output IPC vectors, the node will be removed. The connection weights of neighbor nodes will be adjusted.

**Keeping Step.** If the input IPC as well as output IPC of a hidden node is not equal to the maximum information processing capability (such as Eq. (9)) or the minimum information strength (such as Eq. (10)), the node will be kept.

#### 2.4 The improved LSTM.

The number of hidden nodes is really important because it can directly affect the performance of the neural network. In more detail, if the number of hidden nodes is too small, the learning ability of this network will be weak. Even if the network is able to learn, it will cost a lot of time to train and the training accuracy is very likely to be low. When the number of neurons in the hidden layer is in a reasonable range, increasing the number of neurons can improve the precision of the network training, and may also reduce the number of training. But when it goes beyond that, if the number of neurons is continuing to be increased, the time for network training increases, and it may even cause other problems. So selecting a suitable number of hidden nodes is a vital problem which is difficult to handle. In order to solve this problem, an improved LSTM is proposed. And the flowchart of this work is displayed in Fig. 4.

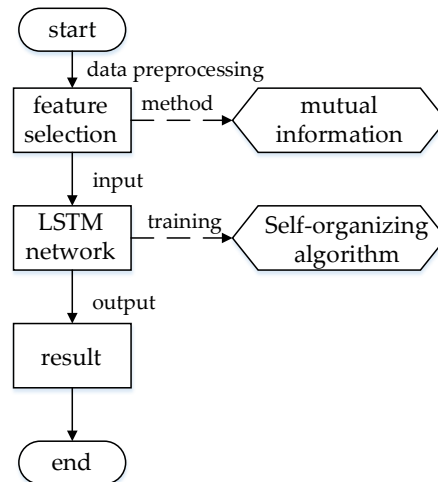


**Figure 4:** Flowchart of this research work

First, at the data preprocessing stage, a method called mutual information is used to select some features, which have a significant impact on  $PM_{2.5}$  concentration. Second, these features are as input data for LSTM neural network. During the training period, a self-organizing algorithm called growing and pruning method is adopted to decide the most suitable number of nodes of the hidden layer. Finally, after training and testing, the result, that is, the predicting  $PM_{2.5}$  concentration is as output of the neural network.

### 3 Experiment

In order to predict the concentration of  $PM_{2.5}$  comprehensively and accurately, not only the hourly precise prediction but also the daily longer-term prediction is taken into account.

#### 3.1 Data preprocessing

To predict  $PM_{2.5}$  concentration, this study uses hourly and daily files of Nanjing, which include meteorological data as well as air pollutants. The meteorological data were collected from Meteorological Data Center of China Meteorological Administration, and the data sources of air pollutants were from Environmental Monitoring Stations of China. The meteorological data and pollution data were collected from the same stations, namely, Maigao Bridge, Caochang Gate, Shanxi Road, Zhonghua Gate, Ruijin Road, Xuanwu Lake, Pukou, Olympic Sports Center and Xianlin University City. Then data were averaged before experiment. Fig. 5 displays a map of the location of each station.

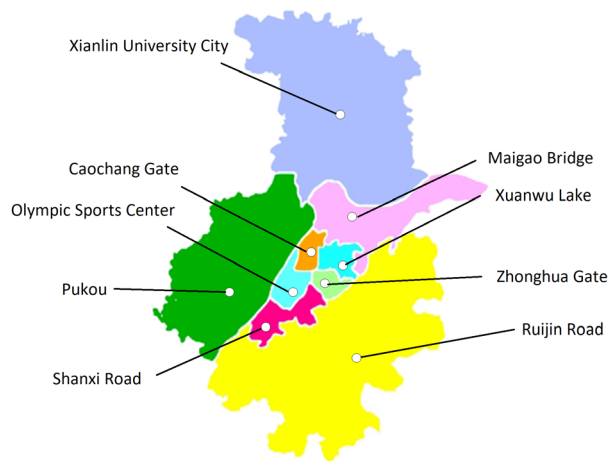


**Figure 5:** Distribution of stations

These nine stations are distributed in all districts of Nanjing, so the average value well reflects the overall  $PM_{2.5}$  level of Nanjing.

##### 3.1.1 Singular value and missing value processing

There are 2664 records in the hourly dataset, and the time interval for the volume of data is one hour. And there are 1320 records in the daily dataset, where the range is from May

13<sup>th</sup> in 2014 to December 31<sup>st</sup> in 2017, and each value is the average value of a day. Raw data contains 27 factors, such as O<sub>3</sub>, NO<sub>2</sub>, CO, SO<sub>2</sub>, pressure, relative humidity, temperature and so on. These meteorological data and pollutant data do not change smoothly, but randomly. However, in the process of recording and calculating, there are some error values (like “937772(μg/m<sup>3</sup>)”). Also there are some missing values. these values will affect the performance of prediction. In order to avoid this problem, this paper uses the average values of neighbor data to replace these values.

### 3.1.2 Feature selection

Then, after the standardization, in order to select the main factors with respect to PM<sub>2.5</sub> concentration, a selection method called Mutual Information (MI) is adopted. Claude Shannon, a famous mathematician, pioneered the information theory in the middle of the 20th century and put forward a key concept-entropy, which is used to measure the uncertainty of a given probability distribution. MI is a method in information theory. It mainly calculates how much influence one thing has on the appearance of another. It is a measurement method for calculating how much information one attribute feature contains another attribute feature. The formula of mutual information is as follows

$$MI(X; Y) = \sum_{x \in X} \sum_{y \in Y} p(x, y) \log \frac{p(x, y)}{p(x)p(y)} \quad (11)$$

$p(x, y)$  is the joint distribution of two characteristic variables  $x$  and  $y$ , and  $p(x)$  and  $p(y)$  represent the marginal distribution of two characteristic variables respectively.

This method can calculate that whether there is a relationship between the two variables  $X$  and  $Y$ , as well as the strength of the relationship. As a result, the MI values of these factors are high: O<sub>3</sub>, NO<sub>2</sub>, PM<sub>2.5</sub>, pressure, windy speed of instant maximum, wind direction of instant maximum, temperature, wind direction of maximum wind speed, relative humidity, water vapor pressure, minimum relative humidity, horizontal visibility, and body temperature.

### 3.2 Verification and validation

Through Section 3.1.2, several features were selected by a feature selection method. These features are as input data for LSTM neural network, which are O<sub>3</sub>, NO<sub>2</sub>, PM<sub>2.5</sub>, pressure, windy speed of instant maximum, wind direction of instant maximum, temperature, wind direction of maximum wind speed, relative humidity, water vapor pressure, minimum relative humidity, horizontal visibility, and body temperature. Learning rate is set to be 0.1, loss function is Mean Absolute Error (MAE).

$$MAE = \frac{1}{m} \sum_{i=1}^m |y - \bar{y}| \quad (12)$$

$m$  is the number of samples,  $y$  is the monitoring value and  $\bar{y}$  is the predicted value.

*3.2.1 Hourly prediction*

For hourly prediction, the model is fit for 500 training epochs, the dataset is splitted into training, validating and testing sets, training set is set to be 2000 records, validating set is set to be 563 and testing set is set to be 100 records.

To prove that the number of hidden nodes decided by the self-organizing algorithm is the most suitable one, some different numbers of hidden nodes are used for comparison. Tab. 1 shows the result of predicting PM<sub>2.5</sub> concentration after 1 hours, 4 hours, 8 hours and 12 hours.

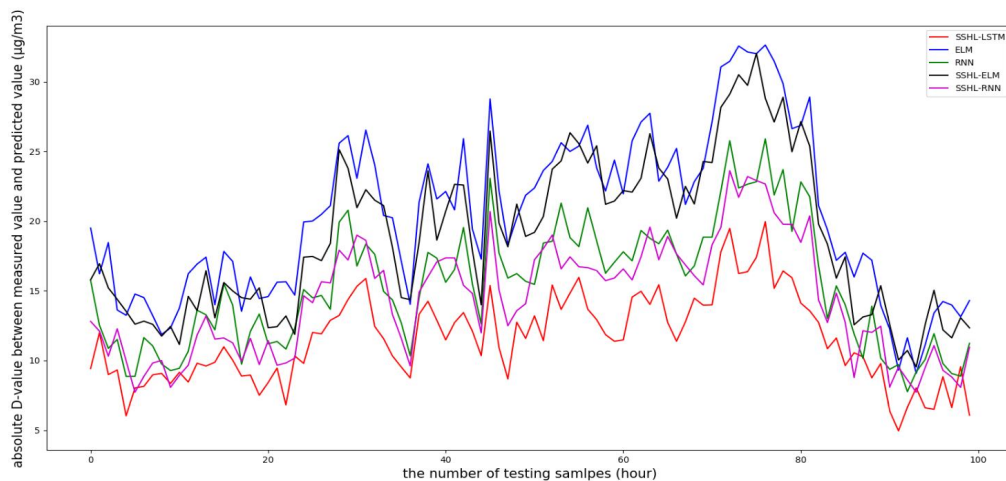
**Table 1:** The hourly predicting comparison between different numbers of hidden nodes

Future Hours	Number of Hidden	Accuracy Rate (%)
1	5	93.378
	6	93.022
	7	93.257
	<b>8</b>	<b>93.396</b>
	9	93.295
	10	93.205
	15	93.222
	18	93.257
4	20	93.141
	5	86.944
	6	86.831
	7	86.826
	<b>8</b>	<b>87.134</b>
	9	86.814
	10	86.437
	15	86.748
8	18	86.277
	20	86.431
	5	85.917
	6	85.792
	7	85.870
	<b>8</b>	<b>86.086</b>
	9	86.044
	10	85.897
12	15	85.716
	18	85.372
	20	85.641
	5	84.617
12	6	84.097
	7	84.983

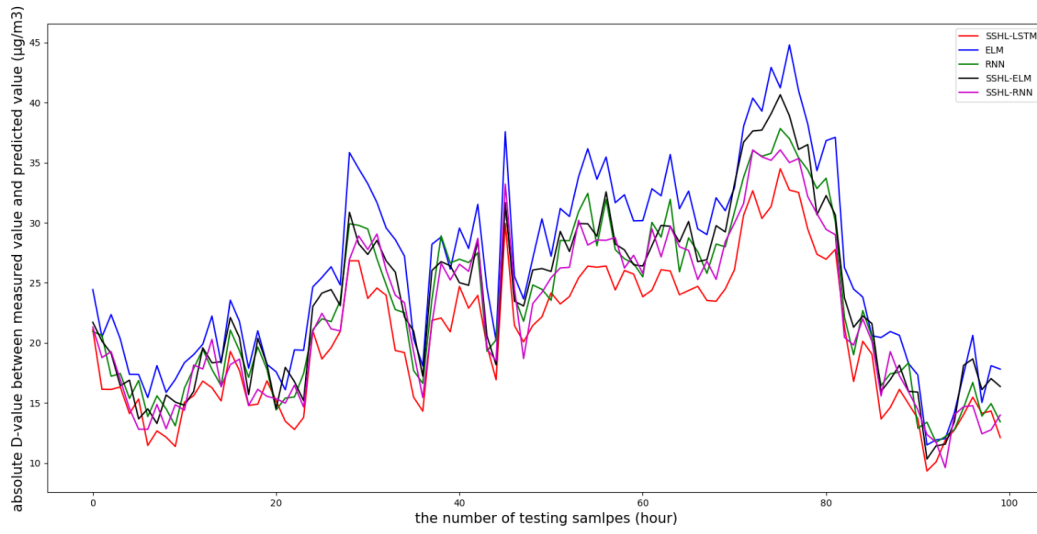
<b>8</b>	<b>85.916</b>
9	84.979
10	85.037
15	85.082
18	84.793
20	84.985

According to the self-organizing algorithm, the number of hidden nodes is determined to be 8. From Tab. 1, when prediction interval time is set to be 1 hour, 4 hours, 8 hours and 12 hours, the correlation rates of 8 hidden nodes are the highest when compared with other number of hidden nodes. So the self-organizing algorithm is proved to be effective. Also, according to this table, the longer the prediction interval is, the lower the accuracy of the prediction will be.

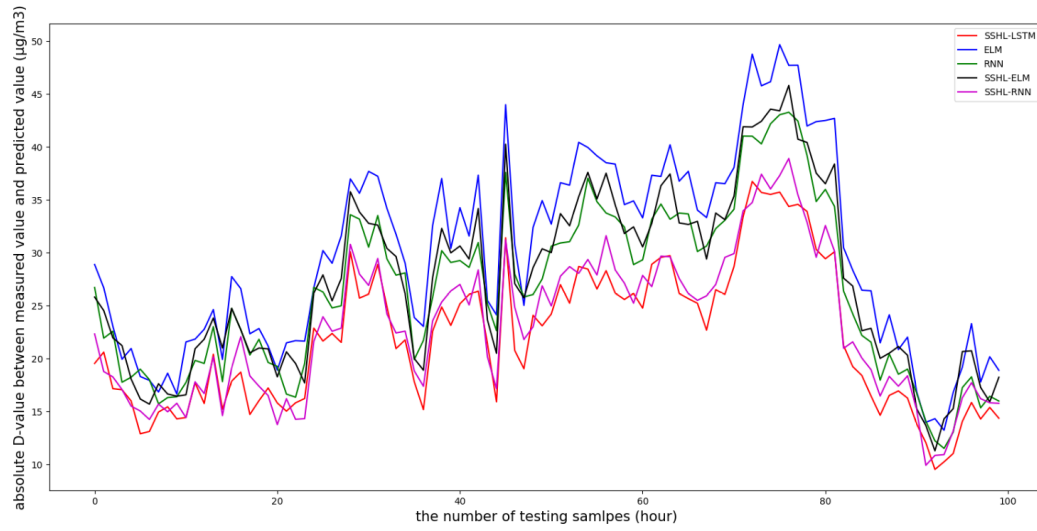
In order to validate the superiority of the SSHL-LSTMNN for hourly prediction, there is a comparison experiment between the SSHL-LSTMNN and other neural networks. From the perspective of network structure, this paper adopts extreme learning machine (ELM), which is a kind of feedforward neural network and recurrent neural network (RNN), which contains a self-feedback structure, to compare with the neural network which is proposed by this paper. In addition, the Self-organizing Single Hidden-Layer ELM (SSHL-ELM) and the Self-organizing Single Hidden-Layer RNN (SSHL-RNN) are used as the comparison benchmarks as well. This experiment adopts these models to predict PM<sub>2.5</sub> concentration of next 1 hour, 4 hours, 8 hours and 12 hours in Nanjing. In Fig. 5, the X-axis is the quantity of the testing samples, and the Y-axis is the absolute Difference-value (D-values) between measured data and predicted data of different models. Red line represents SSHL-LSTM, blue line represents ELM, green line represents RNN, black line represents SSHL-ELM and purple line represents SSHL-RNN.



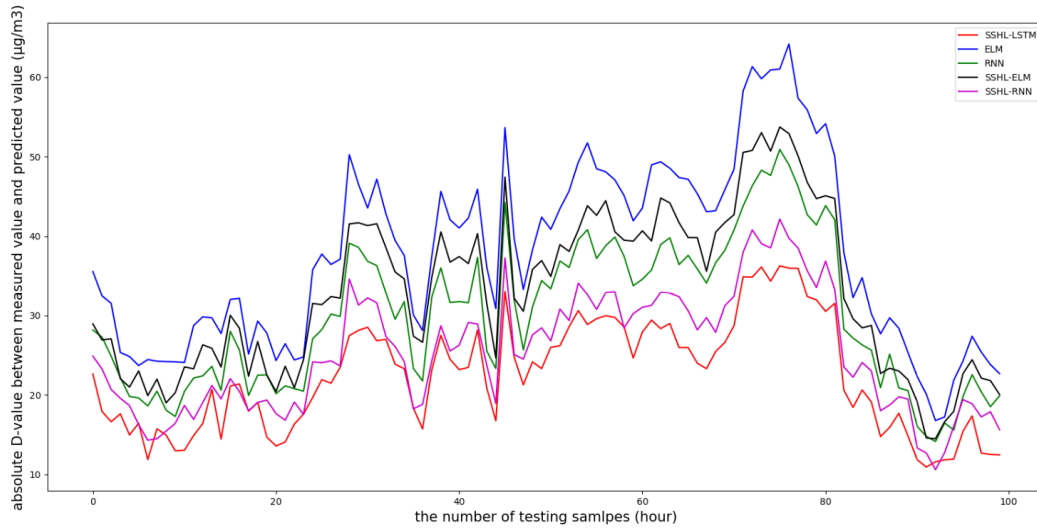
(a) 1 hour



(b) 4 hours



(c) 8 hours



(d) 12 hours

**Figure 6:** Absolute D-values between measured data and predicted data of different models for the testing dataset for one-, four-, eight-, and twelve-hour

From Fig. 6, it can be observed that the red line is always the lowest, which means the absolute D-values between measured data and predicted data of SSHL-LSTM are the smallest. So the prediction accuracy of SSHL-LSTM is proved to be the highest. Though sometimes the curves overlap partially because the predicted values are close, on the whole, the order of prediction accuracy from high to low is: SSHL-LSTM, SSHL-RNN, RNN, SSHL-ELM and ELM. As the time interval lengthens, the prediction accuracy of each model is getting lower. Tab. 2 describes the average predicting correlation rates between different models.

**Table 2:** The hourly predicting comparison between different models

correlation rates / future hours \ models	ELM	RNN	SSHL-LSTMNN	SSHL-ELM	SSHL-RNN
1	87.385%	90.749%	<b>93.396%</b>	88.427%	91.433%
4	83.284%	85.389%	<b>87.134%</b>	84.836%	85.932%
8	80.672%	83.021%	<b>86.086%</b>	82.372%	85.521%
12	75.386%	80.528%	<b>85.916%</b>	78.622%	83.794%

According Tab. 2, the correlation rates of different neural network for PM<sub>2.5</sub> prediction are displayed. Obviously, SSHL-LSTMNN algorithm shows higher correlation rates than ELM, RNN, SSHL-ELM and SSHL-RNN regardless of the time interval. Also, the

prediction accuracy of SSHL-ELM is higher than that of ELM, and SSHL-RNN is higher than RNN. So the self-organizing algorithm is proved to be effective. From the perspective of network structure, ELM is a kind of feed-forward neural network, which has no feedback loop in the network, so it cannot combine values of history moment as input. But the meteorological data and pollutant data this paper used are typical time series data, which means there is a strong correlation between the trend of data and time. So feed-forward neural network is not able to show a good capability for PM<sub>2.5</sub> prediction. Unlike ELM, RNN has feedback loop in its structure. So RNN can store the history data for the future prediction. However, because of the method of weight updating, RNN can't perform well for long-term prediction. So LSTM neural network is proposed for solving this problem. Therefore, LSTM neural network has better capability than feed-forward neural network and recurrent neural network.

*3.2.2 Daily prediction*

For daily prediction, input data are the same as those of hourly prediction. Learning rate is set to be 0.1, loss function is MAE. The model is fit for 300 training epochs, the dataset is splitted into training, validating and testing sets, training set is set to be 1000 records, validating set is set to be 220 and testing set is set to be 100 records.

Hourly prediction can forecast near-time concentration of PM<sub>2.5</sub> instead of daily average concentration. So this section uses daily dataset to evaluate the daily prediction performance. After training by the self-organizing algorithm, the number of hidden neurons is set to be 7. To validate this result, a comparison experiment is operated. The results are shown in Tab. 3.

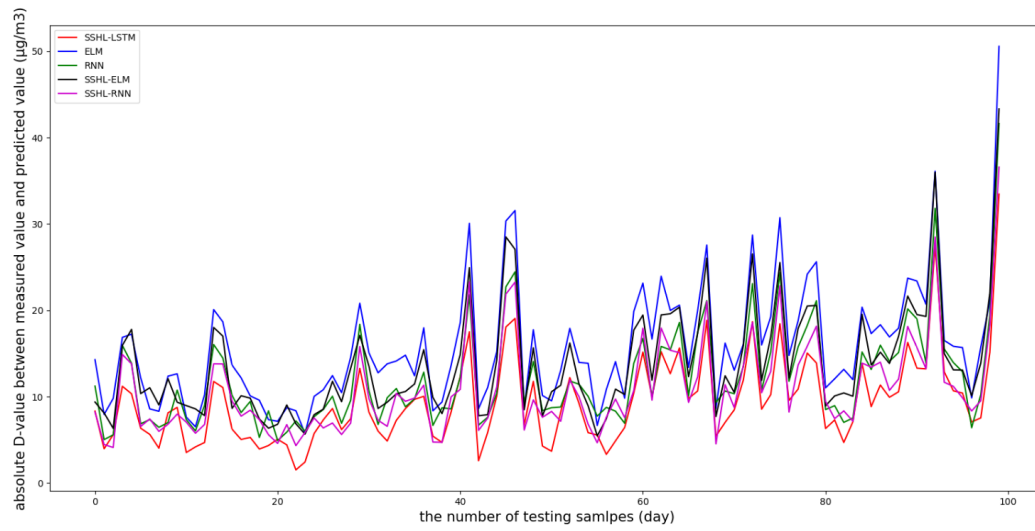
**Table 3:** The daily predicting comparison between different numbers of hidden nodes

Future Days	Number of Hidden Nodes	Accuracy Rate (%)
1	5	79.491
	6	81.182
	<b>7</b>	<b>81.707</b>
	8	81.359
	9	81.427
	10	81.295
	15	81.551
	18	81.466
	20	81.519
4	5	76.928
	6	77.926
	<b>7</b>	<b>78.914</b>

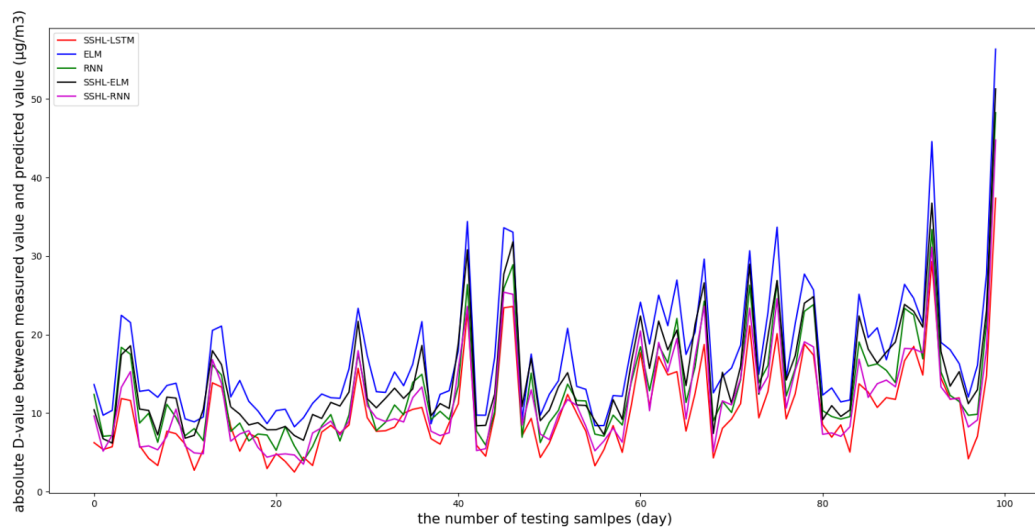
	8	77.561
	9	78.192
	10	77.830
	15	78.391
	18	78.154
	20	78.212
	5	77.191
	6	77.767
	<b>7</b>	<b>78.326</b>
	8	77.585
8	9	78.268
	10	77.875
	15	77.961
	18	77.861
	20	77.971
	5	76.017
	6	76.611
	<b>7</b>	<b>77.190</b>
	8	76.919
12	9	76.049
	10	76.593
	15	75.137
	18	76.172
	20	76.239

According to the self-organizing algorithm, the number of hidden nodes is adjusted to be 7. From Tab. 3, it is obvious that when the number of hidden nodes is 7, correlation rates perform better than other conditions. So the self-organizing LSTM model is proved to be effective. However, comparing with Tab. 1, the prediction accuracy of daily prediction is much lower than hourly prediction. So this method is more applicable for short-term forecasting.

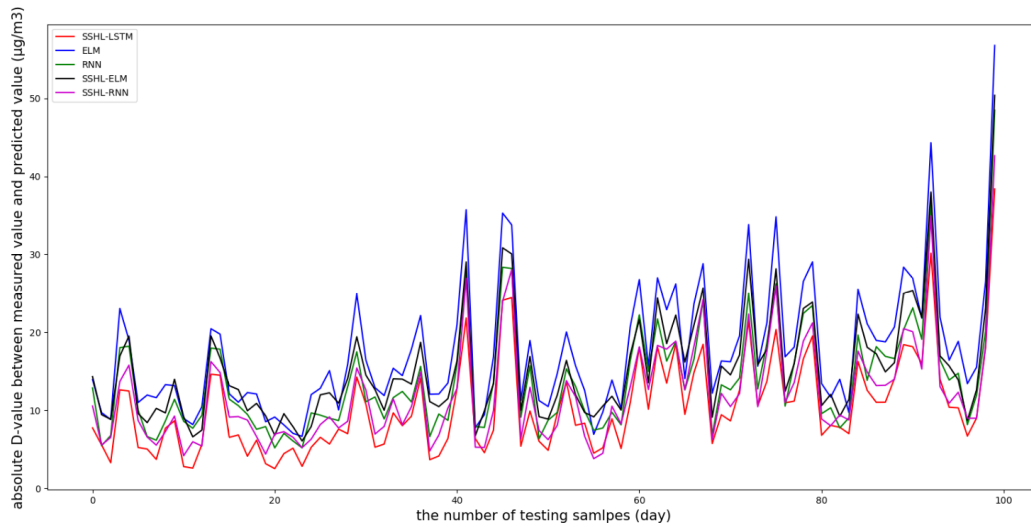
In order to validate the outstanding performance of the proposed model, Fig. 7 shows the displays the curves of the absolute D-values between measured data and predicted data of different models.



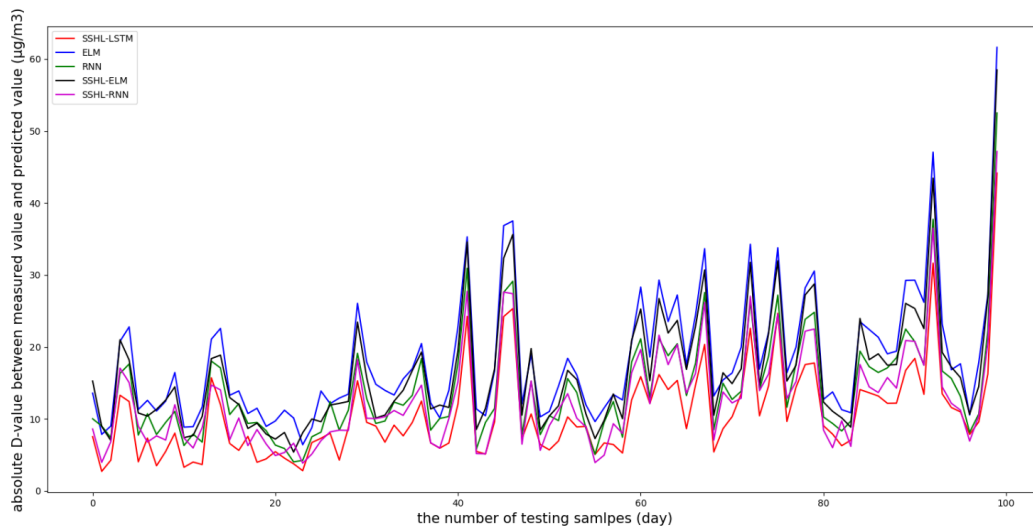
(a) 1 day



(b) 4 days



(c) 8 days



(d) 12 days

**Figure 7:** Actual and predict  $PM_{2.5}$  concentration for the evaluation dataset for one-, four-, eight-, and twelve-day

From Fig. 7, it can be seen that the red line is always the lowest, which means the absolute D-values between measured data and predicted data of SSHL-LSTM are the smallest. So the daily prediction accuracy of SSHL-LSTM is proved to be the highest. Compared to hourly prediction, the clearance of curves of different models is smaller, which means the daily prediction accuracy is closer between different models.

Tab. 4 describes the average predicting correlation rates between different models.

**Table 4:** The daily predicting comparison between different neural networks

correlation rates future days	ELM	RNN	SSHL-LSTMNN	SSHL-ELM	SSHL-RNN
1	75.478%	79.485%	<b>81.707%</b>	77.429%	80.377%
4	71.368%	76.055%	<b>78.914%</b>	74.386%	76.834%
8	70.942%	75.037%	<b>78.326%</b>	73.267%	76.522%
12	68.179%	73.587%	<b>77.190%</b>	70.255%	74.624%

According to Tab. 4, SSHL-LSTMNN also performs best for daily prediction. But compared with Tab. 2, the correlation rates are much lower than hourly prediction. In addition, the changes of correlation rates are not very significant when time interval changes. It may be because the correlation between daily data is not as strong as that between hourly data, so it's difficult to fit the nonlinear relationship between daily data.

## 5 Conclusion and future work

Because meteorological data and pollutant data are typical time series data, LSTM network is suitable to apply in this case for its memory capability. Therefore, this paper proposed a machine learning method, an improved LSTM neural network to predict hourly and daily PM<sub>2.5</sub> concentration. The improved LSTM neural network was trained by a self-organizing algorithm, which solved the problem that the number of hidden layer nodes was difficult to determine. Experimental results verified the superiority of the SSHL-LSTMNN algorithm.

For future work, topographic condition and weather condition should be taken into account. For example, Nanjing is surrounded by mountains on three sides, the terrain is typical "dustpan" shape. It is easy to form unfavorable meteorological conditions such as static wind and inversion temperature. The diffusion conditions of atmospheric pollutants are poor. Especially in autumn and winter, it is easy to have continuous and steady foggy weather, which leads to moderate and severe pollution. More different topographic conditions like plateau and Plain can be researched in the future.

**Acknowledgement:** This work was supported by Scientific Research Project of The Education Department of Hunan Province (Grant No. 17C0479) and Marie Curie Fellowship (701697-CAR-MSCA-IF-EF-ST).

## References

**Bengio, Y.; Simard, P.; Frasconi, P.** (1994): Learning long-term dependencies with gradient descent is difficult. *IEEE Transactions on Neural Networks*, vol. 5, no. 2, pp. 157-166.

**Bun, T.; Komei, S.; Koji, Z.** (2016): Dynamically pre-trained deep recurrent neural networks using environmental monitoring data for predicting PM<sub>2.5</sub>. *Neural Computing & Applications*, vol. 27, no. 6, pp. 1553-1566.

**Dong, M.; Yang, D.; Kuang, Y.** (2009): PM<sub>2.5</sub> concentration prediction using hidden semi-Markov model-based time series data mining. *Expert Systems with Application*, vol. 36, no. 5, pp. 9046-9055.

**El-Sousy, F. F. M.** (2014): Adaptive hybrid control system using a recurrent RBFN-based self-evolving fuzzy-neural-network for PMSM servo drives. *Applied Soft Computing*, vol. 21, no. 1, pp. 509-532.

**El-Sousy, F. F. M.; Khaled, A. A.** (2016): Self-organizing recurrent fuzzy wavelet neural network-based mixed H<sub>2</sub>/H<sub>∞</sub> adaptive tracking control for uncertain two-axis motion control system. *IEEE Transactions on Industry Applications*, vol. 52, no. 6, pp. 5139-5154.

**El-Sousy, F. F. M.; Khaled, A. A.** (2018): Adaptive nonlinear disturbance observer using a double-loop self-organizing recurrent wavelet neural network for a two-axis motion control system. *IEEE Transactions on Industry Applications*, vol. 54, no. 1, pp. 764-786.

**Fuller, G. W.; Carslaw, D. C.; Lodge, H. W.** (2002): An empirical approach for the prediction of daily mean PM<sub>10</sub> concentrations. *Atmospheric Environment*, vol. 36, no. 9, pp. 1431-1441.

**Han, H.; Li, Y.; Guo, Y.; Qiao, J.** (2016): A soft computing method to predict sludge volume index based on a recurrent self-organizing neural network. *Applied Soft Computing*, vol. 38, no. C, pp. 477-486.

**Han, H. G.; Zhang, L.; Hou, Y.; Qiao, J. F.** (2016): Nonlinear model predictive control based on a self-organizing recurrent neural network. *IEEE Transactions on Neural Networks and Learning Systems*, vol. 27, no. 2, pp. 402-415.

**Hochreiter, S.; Schmidhuber, J.** (1997): Long short-term memory. *Neural Computation*, vol. 9, no. 8, pp. 1735-1780.

**Hsu, C. F.** (2014): Adaptive backstepping Elman-based neural control for unknown nonlinear systems. *Neurocomputing*, vol. 136, no. 1, pp. 170-179.

**Jian, L.; Zhao, Y.; Zhu, Y. P.; Zhan, M. B.; Bertolatti, D.** (2012): An application of ARIMA model to predict submicron particle concentrations from meteorological factors at a busy roadside in Hangzhou, China. *Science of the Total Environment*, vol. 426, no. 2, pp. 336-345.

**Liu, D. J.; Li, L.** (2015): Application study of comprehensive forecasting model based on entropy weighting method on trend of PM<sub>2.5</sub> concentration in Guangzhou, China. *International Journal of Environmental Research & Public Health*, vol. 12, no. 6, pp. 7085-7099.

**Mishra, D.; Goyal, P.; Upadhyay, A.** (2015): Artificial intelligence based approach to forecast PM<sub>2.5</sub>, during haze episodes: a case study of Delhi, India. *Atmospheric Environment*, vol. 102, pp. 239-248.

**Park, D. C.** (2013): Structure optimization of BiLinear recurrent neural networks and its application to ethernet network traffic prediction. *Information Sciences*, vol. 237, no. 1, pp. 18-28.

**Subrahmanya, N.; Shin, Y. C.** (2010): Constructive training of recurrent neural networks using hybrid optimization. *Neurocomputing*, vol. 73, no. 13-15, pp. 2624-2631.

**Tsai, Y.; Zeng, Y.; Chang, Y.** (2018): Air pollution forecasting using RNN with LSTM. *IEEE 16th International Conference on Dependable, Autonomic and Secure Computing*.

**Venkadesh, S.; Hoogenboom, G.; Potter, W.** (2013): A genetic algorithm to refine input data selection for air temperature prediction using artificial neural networks. *Applied Soft Computing*, vol. 13, no. 5, pp. 2253-2260.

**Verma, I.; Ahuja, R.; Meisheri, H.; Dey L.** (2018): Air pollutant severity prediction using Bi-directional LSTM Network. *IEEE/WIC/ACM International Conference on Web Intelligence*.

**Vukovic, N.; Miljkovic, Z.** (2013): A growing and pruning sequential learning algorithm of hyper basis function neural network for function approximation. *Neural Networks*, vol. 46, no. 1, pp. 210-226.

**Wang, X. X.; Ma, L. Y.; Wang, B. S.; Wang, T.** (2013): A hybrid optimization-based recurrent neural network for real-time data prediction. *Neurocomputing*, vol. 120, no. 1, pp. 547-559.

**Zheng, H.; Shang, X.** (2013): Study on prediction of atmospheric PM2.5 based on RBF neural network. *Fourth International Conference on Digital Manufacturing & Automation*.

**Zhou, S.; Li, W.; Qiao, J.** (2017): Prediction of PM2.5 concentration based on recurrent fuzzy neural network. *Proceedings of the 36th Chinese Control Conference*.

**Zhu, H.; Lu, X.** (2016): The prediction of PM2.5 value based on ARMA and improved BP neural network model. *International Conference on Intelligent Networking and Collaborative Systems*.